Topology-optimized broadband surface relief transmission grating

Jacob Andkjær*[a], Christian P. Ryder[a], Peter C. Nielsen[a], Thomas Rasmussen[a], Kristian Buchwald[a], Ole Sigmund[b]
[a]Ibsen Photonics, Ryttermarken 17, Farum, Denmark 3520
[b]Dept. of Mechanical Engineering, Technical University of Denmark (DTU), Nils Koppels Allé, Kgs. Lyngby, Denmark 2800

ABSTRACT

We propose a design methodology for systematic design of surface relief transmission gratings with optimized diffraction efficiency. The methodology is based on a gradient-based topology optimization formulation along with 2D frequency domain finite element simulations for TE and TM polarized plane waves. The goal of the optimization is to find a grating design that maximizes diffraction efficiency for the -1st transmission order when illuminated by unpolarized plane waves. Results indicate that a surface relief transmission grating can be designed with a diffraction efficiency of more than 40% in a broadband range going from the ultraviolet region, through the visible region and into the near-infrared region.

Keywords: Transmission grating, topology optimization, diffraction efficiency, broadband spectroscopy

1. INTRODUCTION

Diffraction gratings have been manufactured for over 200 years, with developments driven initially by requirements of spectroscopy, where gratings have been applied ever since Joseph von Fraunhofer's work in the early 1800's. Over the past decades, semiconductor technology has appeared and matured, offering manufacturing technologies applicable to transmission gratings, and bringing with it the high-volume, low-cost benefits of semiconductor technology. For this reason, dielectric transmission gratings have found widespread use in the ultraviolet, visible and near-infrared spectral ranges during the past 5-10 years. These applications rely on grating structures with high diffraction efficiency for the specific setup. However, it is very challenging to find efficient grating structures that are efficient from the ultraviolet to the near-infrared, due to the diffraction efficiency having a non-trivial dependency on the material distribution of the grating. In this work we propose a design procedure for systematic design of broadband surface relief transmission gratings with optimized diffraction efficiency.

Diffraction gratings can be divided into reflection gratings or transmission gratings depending on whether they reflect an incident wave or transmit it through the grating. Reflection gratings are very sensitive to the incident angle and therefor i.e. difficult to align in a spectrometer. In contrast, transmission gratings are very robust to variation in incident angle. Furthermore, reflection gratings have in general lower diffraction efficiency than transmission gratings due to the inherent loss in the metal surface. Surface relief gratings and volume phase gratings are the two common types of transmission gratings in use. Surface relief gratings can be manufactured by etching into the surface of a glass substrate using a mask layer to define the periodic pattern. Volume phase gratings are typically manufactured in a dichromated gelatin that is sandwiched between two glass substrates. The refractive index of dichromated gelatin can be changed permanently by illumination with laser light, and thus by illuminating the material with an interference pattern, a permanent periodic index modulation is created. Surface relief gratings generally have strong index modulation, while volume phase gratings have weak index modulation. As a result, volume phase gratings are generally thick gratings and have smaller bandwidth [1] compared to surface relief gratings, which are thin gratings with larger bandwidth. The dichromated gelatin in volume phase gratings is transparent from ~350 nm through the near-infrared, so volume phase gratings can generally not be made for the ultraviolet spectrum. In contrast, surface relief gratings based on fused silica can be made for any wavelength range from ultraviolet through near-infrared. Hence we focus our study on surface relief transmission gratings in order for the grating to be effective below 350 nm.

*Jacob.andkjaer@ibsen.dk; phone +45 4434 7022; www.ibsenphotonics.com

Physics and Simulation of Optoelectronic Devices XXII, edited by Bernd Witzigmann, Marek Osinski, Fritz Henneberger, Yasuhiko Arakawa, Proc. of SPIE Vol. 8980, 898006 · © 2014 SPIE
CCC code: 0277-786X/14/$18 · doi: 10.1117/12.2036997

The dielectric layout of the periodic structure in the surface relief grating determines how much energy of the incident wave is distributed in the existing transmission orders. However, as mentioned, it is very challenging to find grating structures that are efficient from the ultraviolet to the near-infrared, due to the diffraction efficiency having a non-trivial dependency on the material distribution of the grating. Previous studies have analyzed and optimized the diffraction properties for various surface relief transmission grating profiles such as binary [1-8], sinusoidal [1, 2], triangular [1, 9], blazed [2, 9] and buried gratings [10,11]. Though many of the presented grating designs are highly efficient, they are in most cases only designed to operate at a specific polarization (often TE), and their bandwidths are below ~200 nm. In Ref. 6 it is demonstrated that it is also possible to design surface relief gratings with diffraction efficiency above 97% for unpolarized illumination, but with a limited bandwidth. In the above studies all the grating profiles have a rather simple geometrical shape. In this study we want to lay out a systematic procedure to find grating designs with novel geometries without any geometrical restrictions.

Several studies [12-14] have shown that using layers of different dielectric materials and even thin layers of metal in the grating design can enhance the diffraction efficiency of surface relief gratings. Layered design adds more design freedom, which in many cases makes it easier to manipulate the transmitted wave to propagate in the direction of the -1st order. However, it is very challenging to find materials with insignificant loss in the entire frequency range going from ultra-violet to near-infrared (especially in the ultraviolet frequency range). For this reason we have limited our grating design only to consist of fused silica.

In previous studies [15–17], a method based on topology optimization [18] has been formulated for designing nanostructured periodic surfaces with extreme reflection or transmission properties. The method can even be used for designing nanostructured multilayered surfaces displaying prescribed structural color properties [19]. Here we extend the initial study by including a near- to far-field transformation of the transmitted wave and converting the transmitted far-field to diffraction efficiency. With this extension we obtain a procedure based on topology optimization for designing surface relief transmission gratings with optimized diffraction properties.

Topology optimization is a gradient based optimization method that redistributes material in a bounded design domain in order to optimize certain responses of the physical system (e.g. maximize diffraction efficiency). The analysis for finding the diffraction efficiency for a given grating design is performed with the finite element method [20] in this study. Other numerical tools such as the finite difference method [21] could likewise have been used. The topology optimization method was originally developed for mechanical design problems [18, 22] but has since then been extended to a number of other physics areas including nano-photonics [23–25], antennas [26] and meta-materials [27]. The power of this optimization method is that it can suggest novel designs without any geometrical restrictions. However, the optimized designs may contain many small details and will therefore be very challenging to fabricate. In order to get designs that are simpler to fabricate, one may introduce geometrical constraints in the optimization problem as e.g. seen in Ref. 17, where a connectivity constraint in the grating design is introduced. Another workaround is to construct a simplified design based on the optimized complex design. Obviously, imposing constraints on the geometrical freedom or simplifying an optimized design come at the cost of limiting the achievable diffraction efficiency.

The rest of the paper is organized as follows. Section 2 describes the finite element modeling procedure, the near- to far-field mapping, as well as the calculation of the diffraction efficiency based on the far-field. Section 3 describes the design procedure and the optimization problem. Section 4 discusses the optimized surface relief transmission grating with maximized diffraction efficiency for the -1st order in the ultraviolet to near infrared spectrum. Section 5 concludes on the work.

2. MODELING OF SURFACE RELIEF TRANSMISSION GRATINGS

2.1 Numerical model

The numerical setup is similar to previous studies [17, 19] on reflection-type gratings but here extended to work for a broadband transmission grating with a dispersive material model. We consider the two fundamental modes of linear polarization. Assuming invariance of the electromagnetic properties in the out-of-plane direction, Maxwell's equations simplify to the scalar Helmholtz equation. The scalar Helmholtz equation governs the physics for steady-state electromagnetic wave problems with a sinusoidal transverse electric (TE) or transverse magnetic (TM) polarized plane wave of angular frequency ω using $\exp(j\omega t)$ to convert from phasor to time notation. The electric field E_z is parallel to the grooves and perpendicular to the plane (x, y) of propagation in the TE polarization. Here we state the governing

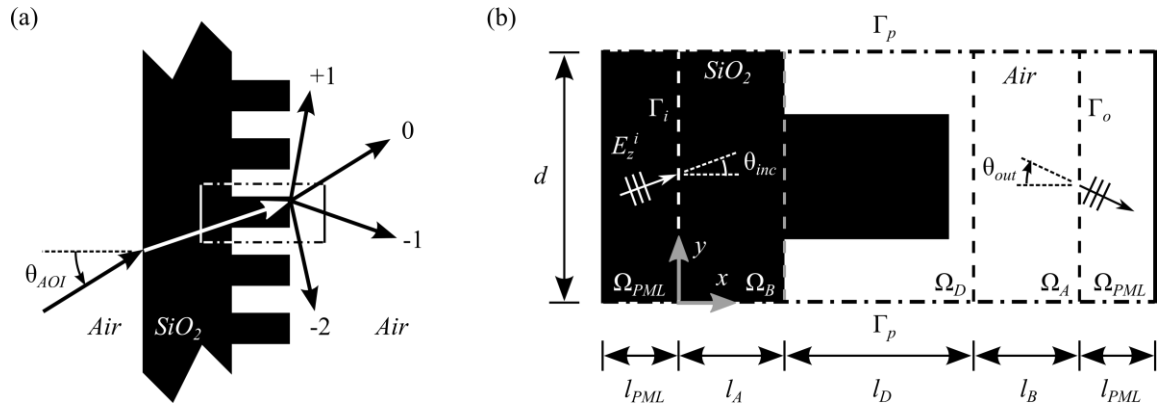

Figure 1: a) A surface relief transmission grating diffracts an incident plane wave. b) The computational domain is simplified to one period using periodic boundaries and truncated using perfect matching layers.

equation for a TE polarized wave. Equivalent equations for the TM polarization are easily obtained by interchanging $E_z \leftrightarrow H_z$ and $\varepsilon_r \leftrightarrow \mu_r$. The scalar Helmholtz equation is given as

$$\nabla \cdot \left(\mu_r^{-1} \nabla E_z\right) + k_0^2 \varepsilon_r E_z = 0, \tag{1}$$

where ε_r is the relative permittivity, μ_r is the relative permeability, and $k_0 = \omega/c$ is the free space wave number. A sketch of a surface relief transmission grating with a grating period of d is shown in Fig. 1(a). A plane wave is assumed incident at an angle θ_{AOI} on the grating. Due to the periodicity along the y-axis we can simplify the numerical analysis by modeling a domain of one period with periodic boundaries at Γ_p as sketched in Fig. 1. The domain is furthermore truncated at the left and right boundaries using perfectly matched layers (PML) [20]. The governing equation in the PML regions is

$$\frac{\partial}{\partial x}\left(\frac{s_y}{s_x}\mu_r^{-1}\frac{\partial E_z}{\partial x}\right) + \frac{\partial}{\partial y}\left(\frac{s_x}{s_y}\mu_r^{-1}\frac{\partial E_z}{\partial y}\right) + k_0^2 s_x s_y \varepsilon_r E_z = 0, \tag{2}$$

where s_x and $k_0 = \omega/c$ are complex functions of the position and govern the damping properties of the PML. Thus the computational domain is given in 2D and consists of three main regions: a bulk (substrate) region Ω_B; a grating (design) region Ω_D and an air region Ω_A, see Fig. 1. By truncating the grating structure this way it furthermore implies that the reflection on the backside of the substrate is omitted in the numerical work. We assume in other words, that the backside of the substrate is coated with a perfect anti-reflection coating. The incident field E_z^i is given as

$$E_z^i = E_{z0} \exp\left(-jk_0\sqrt{\varepsilon_r \mu_r}\hat{\mathbf{k}} \cdot \hat{\mathbf{r}}\right), \tag{3}$$

where E_{z0} is the amplitude of the wave, $\hat{\mathbf{k}} = \left(\hat{k}_x, \hat{k}_y\right)^T$ is the normalized directional wave vector and $\hat{\mathbf{r}} = (x, y)^T$ is the spatial position vector. The incident wave is generated by a surface electric current density $\mathbf{J}_s$ on the boundary Γ_i only having a z-component given by

$$J_{sz} = 2\cos(\theta_{inc})\sqrt{\frac{\varepsilon_0 \varepsilon_r \mu_r}{\mu_0}} E_z^i, \tag{4}$$

where θ_{inc} is the angle of the incoming wave to the normal of Γ_i. The angle of the incoming wave in fused silica can easily be derived from the angle of incidence in air using Snell's law

$$\sin(\theta_{inc}) = \frac{1}{\sqrt{\varepsilon_r^{SiO_2}(\lambda)}} \sin(\theta_{AOI}), \tag{5}$$

where $\varepsilon_r^{SiO_2}$ is the wavelength dependent relative permittivity of fused silica (SiO_2). The Sellmeier equation models the dispersive behavior of fused silica in the following way

$$\varepsilon_r^{SiO_2}(\lambda) = 1 + \frac{0.696166\lambda^2}{\lambda^2 - 0.00467915} + \frac{0.407943\lambda^2}{\lambda^2 - 0.0135121} + \frac{0.897479\lambda^2}{\lambda^2 - 97.934}. \tag{6}$$

where λ is the wavelength in micrometers. The periodic boundary on Γ_p are given by the Bloch-Floquet condition

$$E_z(x,d) = E_z(x,0)\exp\left(-j\omega\sqrt{\varepsilon_r\mu_r}\, d\sin(\theta_{in})\right). \tag{7}$$

The problem is solved using the finite element method (FEM) [20] and discretization details can be found in [17]. The field in close proximity and inside the grating structure is found with the solution of the FEM problem. However, the transmitted wave will most likely propagate a distance equal to many wavelengths before reaching a detector. Hence, the field of interest is the far-field and not the near-field found from the FEM solution. To accommodate this, a near- to far-field transformation is performed on the radial component of the scattered field based on Huygen's principle [20] and discarding any terms that decay faster than $1/\sqrt{\rho}$ where ρ is the observation distance. The radial component of the scattered far-field E_z^{sr} can be extracted from the near-field using the following expression from Ref. 20 p. 17

$$E_z^{sr}(\rho,\lambda,\theta_{out}) \approx \sqrt{\frac{jk_0}{8\pi\rho}}\exp(-jk_0\rho)\int_0^d \left[\left(\hat{n}_y\sin(\theta_{out}) + \hat{n}_x\cos(\theta_{out})\right)E_z^s - \frac{1}{jk_0}\left(\hat{n}_x\frac{\partial E_z^s}{\partial x} + \hat{n}_y\frac{\partial E_z^s}{\partial y}\right)\right]\ldots \exp\left(jk_0\left(x\cos(\theta_{out}) + y\sin(\theta_{out})\right)\right)dy \tag{8}$$

where $E_z^s = E_z - E_z^i$ is the scattered field, θ_{out} is the observation direction, $\hat{n}_x$ and $\hat{n}_y$ are the unit normal vector components at the boundary Γ_o. Note that the line integral along the boundary Γ_o in Eq. (8) is only defined along the y - axis, because the line for Γ_o is constant with respect to x. The observation direction θ_{out} of interest in this study is the propagation direction θ_{-1T} of the -1st order transmitted wave. Thus the transmitted diffraction efficiency η in the transmitted -1st order is found as

$$\eta(\lambda,\theta_{-1T}) = \frac{\rho\lambda}{\cos(\theta_{inc})\cos(\theta_{-1T})}\frac{\left|E_z^{sr}(\rho,\lambda,\theta_{-1})\right|^2}{\left|E_z^i(\lambda)\right|^2}, \tag{9}$$

where θ_{-1} is the angle for the transmitted -1st order derived from the grating equation

$$\sin(\theta_m) = \sin(\theta_{inc}) + \frac{m\lambda}{d}, \tag{10}$$

where m is the m^{th} diffraction order and θ_m is the diffraction angle of the m^{th} diffraction order in air. In Eq. (8) we have multiplied with ρ in order to make the diffraction efficiency independent of the observation distance. Note that the propagation direction θ_{-1T} of the -1st order diffracted wave is affected by wavelength and period but not by the geometrical shape of the grooves.

The numerical model including far-field transform was tested against analytical solutions for structures such as a cylinder as well as numerical solutions from commercial software such as GSOLVER.

3. TOPOLOGY OPTIMIZATION PROCEDURE

3.1 Material distribution by topology optimization

Light can be reflected and/or refracted at interfaces between two media depending on the spatial placement and distribution of the material properties (ε_r and μ_r). Hence, control of these material properties allows wave manipulation for enhancing desirable optical responses, e.g. creating transmission gratings with optimized diffraction efficiency for specified diffraction orders. We employ a standard density-based topology optimization method [24] and restrict our investigations to nonmagnetic materials ($\mu_r = 1$). The optimization method works by varying the distribution of materials within a bounded design domain in order to optimize certain responses of the physical system. We use fused silica as dielectric material for the substrate and grating structure due to its low loss in the ultraviolet region. However, the developed topology optimization methodology can handle any simple (linear, homogeneous, isotropic) material combinations including metallic structures [28]. The relative permittivity in the (grating) design domain Ω_D between air and substrate can be varied continuously on an element basis between the relative permittivity for air $\varepsilon_r^{air} = 1$ and fused silica $\varepsilon_r^{SiO_2}(\lambda)$ given in Eq. (6) above. A continuous design variable $\gamma \in [0;1]$ is introduced for each element in the design domain Ω_D and controls the element material properties. Here γ_e corresponds to air and $\gamma_e = 1$ corresponds to fused silica

$$\varepsilon_r(\gamma_e, \lambda) = \varepsilon_r^{Air} + \gamma_e\left(\varepsilon_r^{SiO_2}(\lambda) - \varepsilon_r^{Air}\right) \tag{11}$$

The continuous design variable formulation allows us to solve the optimization problem with efficient gradient-based design updates [29]. In principle, the optimization may result in "grey-scale" results, i.e. elements that neither corresponds to air nor to fused silica, however, the robust design formulation developed in Refs. 30 and 31 and also used in [17, 19] ensures almost discrete designs through a continuation strategy.

3.2 Optimization problem

The idea of the design procedure is to optimize the diffraction efficiency for the transmitted -1st order from a surface relief grating illuminated by an unpolarized plane wave. The diffraction efficiency of an unpolarized wave with a given wavelength is calculated as the average, $\eta = (\eta_{TE} + \eta_{TM})/2$, of the diffraction efficiency from both the TE and TM polarized waves. Furthermore, the diffraction efficiency is calculated with a resolution of 10 nm in the prescribed wavelength range (190nm – 1100nm). The optimization problem is formulated as a *maxmin* formulation, that is, the lowest diffraction efficiency in the frequency (wavelength) range is maximized. This reduces the risk of the diffraction efficiency dropping to 0% for any frequency in the desired range. Furthermore, a volume constraint is imposed to prevent congestion in the design domain. The optimization problem maximizing the lowest diffraction efficiency in the prescribed wavelength range (190nm – 1100nm) is formulated as

$$\begin{aligned} \max_{\gamma} \ \Phi \ &= \ \min_{k=1,\ldots,N} \frac{\eta_{TE}(\lambda_n, \theta_{-1T}) + \eta_{TM}(\lambda_n, \theta_{-1T})}{2} \\ \text{s.t.} \quad & \frac{1}{V_{\Omega_D}} \int_{\Omega_D} \gamma \, d\Omega_D - \beta \le 0, \qquad 0 \le \gamma \le 1 \end{aligned} \tag{12}$$

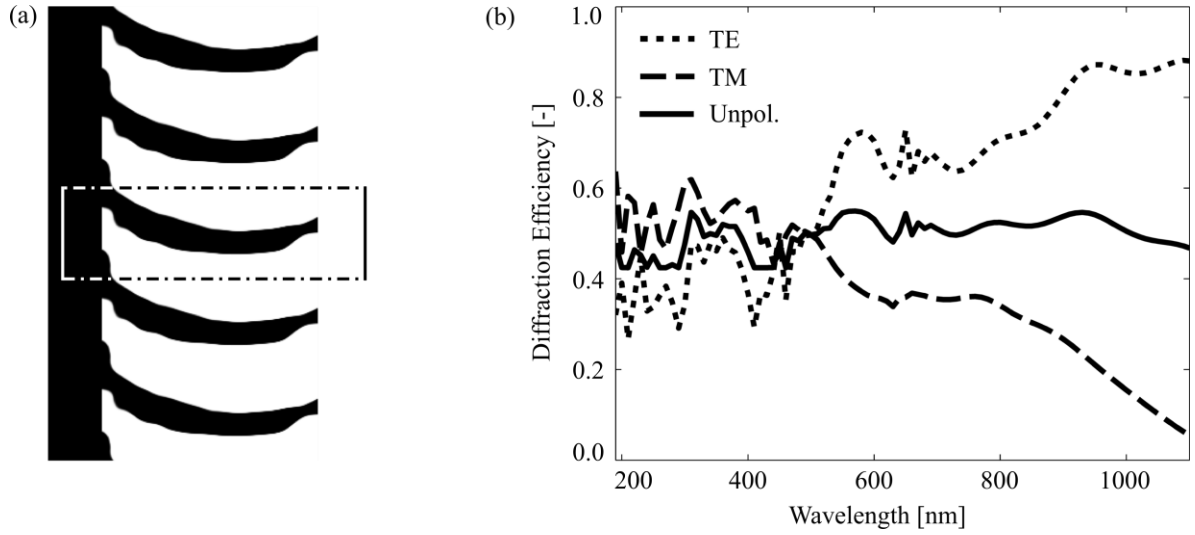

Figure 2: The topology optimized dielectric transmission grating design (a) has been repeated over 5 periods for the purpose of illustration. The black structure represents the grating structure and white represents regions with air. The actual computational domain for one period is shown in the sketched rectangular domain. The resulting diffraction efficiency (b) for the optimized grating in the -1st transmission diffracted direction illuminated by an unpolarized plane wave is above 40% for wavelengths between 190 nm to 1100 nm.

where k is the index of the N angular directions, V_{Ω_D} is the total volume of the design domain Ω_D, and β is the admissible volume fraction. One might introduce manufacturability as a part of the optimization problems by introducing a connectivity constraint (e.g. Ref. 17) to avoid non-connected dielectric "islands" in the grating design. As it turns out this is not needed in the presented example and thus to avoid unnecessary computational work the connectivity constraint has been omitted here.

The design is updated iteratively using the gradient-based optimization routine Method of Moving Asymptotes (MMA) [32]. The lowest diffraction efficiency for the unpolarized wave given as Φ in Eq. (12) is used as a performance measure for the grating design and the sensitivities are obtained using the adjoint method [21]. Convergence is typically reached after 200 to 400 material redistribution steps. We have not utilized parallel computations for the frequency sweeps. However, by doing so, the computational time could easily be reduced.

4. RESULTS

We consider a periodically repeated design domain Ω_D (c.f. Fig. 1). The period is $d = 830\,\text{nm}$ and the thickness is $l_D = 2000\,\text{nm}$. The design domain is discretized with 200×83 finite elements and a maximum of $\beta = 65\%$ of fused silica can be distributed in the design domain. The angle of incidence in air is $\theta_{AOI} = 30°$ and the propagation direction of the -1st transmission order in air varies between $\theta_{-1T} = 15.7°$ for $\lambda = 190\,\text{nm}$ and $\theta_{-1T} = -55.6°$ for $\lambda = 1100\,\text{nm}$.

The optimized design for the broadband surface relief grating obtained using the described methodology is presented in Fig. 2(a). The depth of the grating is 2000nm meaning that the optimizer makes full use of the design domain. Extending the design domain beyond the 2000 nm would most likely improve the diffraction efficiency at the cost of increased complexity in the fabrication. The resulting diffraction efficiency for the optimized grating in the -1st transmission diffracted direction is presented in Fig. 2(b). The optimized grating illuminated by an unpolarized plane wave results in a diffraction efficiency above 40% for wavelengths between 190 nm to 1100 nm. However, a high difference in diffraction efficiency (polarization dependent loss) for TE and TM polarization is seen at wavelengths above 600 nm approximately. At $\lambda = 1100\,\text{nm}$, the efficiency for TE polarization is close to 90%, whereas for TM polarization it is below 10%. In case a high polarization dependent loss is undesirable, it may be circumvented by adding a constraint on the difference in efficiencies for the two polarizations in the optimization problem. Furthermore, the

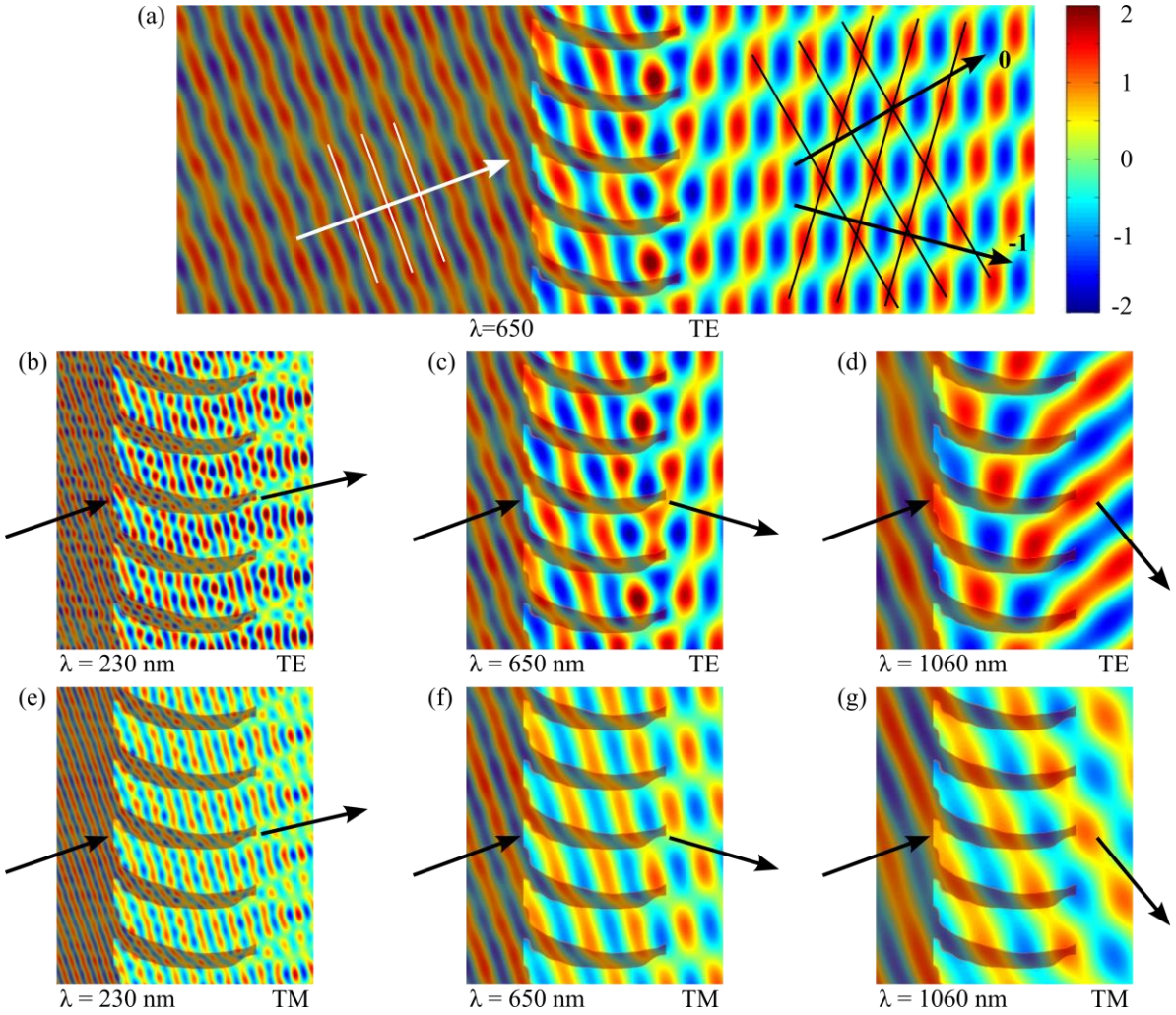

Figure 3: Field plots (5 periods) of TE/TM polarized plane waves with wavelength of 230 nm, 560 nm and 1060 nm incident on the topology optimized grating structure. A semi-transparent overlay of the grating design is added to the field plots in order to show the wave propagation inside the grating and in close vicinity. The top panel (a) shows a field plot for a TE polarized wave with a wavelength of 560 nm where the interference fringes in the overlapping waves for the 0^{th} and -1^{st} transmission order is clearly seen. Panel (b)-(d) and (e)-(f) show the field plots for TE and TM polarized waves, respectively. The propagation direction of the incident wave and the -1^{st} transmission order is indicated with black arrows.

objective could also be changed from maximizing the unpolarized spectrum to maximizing the smallest efficiency of the two.

The resulting total fields for either TE or TM illumination at three different wavelengths (230 nm, 560 nm and 1060 nm) are shown in Fig. 3. A semi-transparent overlay of the grating design is added to the field plots in order to show the wave propagation inside the grating and in close proximity. The top panel (a) in Fig. 3 shows a wider field plot for the TE polarized wave with a wavelength of 560 nm. Here it is clearly seen how two overlapping waves with propagation direction in the 0^{th} and -1^{st} transmission order are formed after the incident wave exits the grating. The diffraction efficiency is approximately 40% and 60% for the 0^{th} and -1^{st} order, respectively. The black arrows in Figs. 3(b)-3(g) indicate the direction of the incident wave and the -1^{st} transmission order. The task of designing an ultra-broadband gratings is very challenging both for the big difference in the ratio between grating size and wavelength (i.e. how many cycles the wave propagate in grating region), the dispersive behavior of the material and not least the big span in propagation direction of the -1^{st} transmission order (c.f. black arrows in Figs. 3(b)-3(d)).

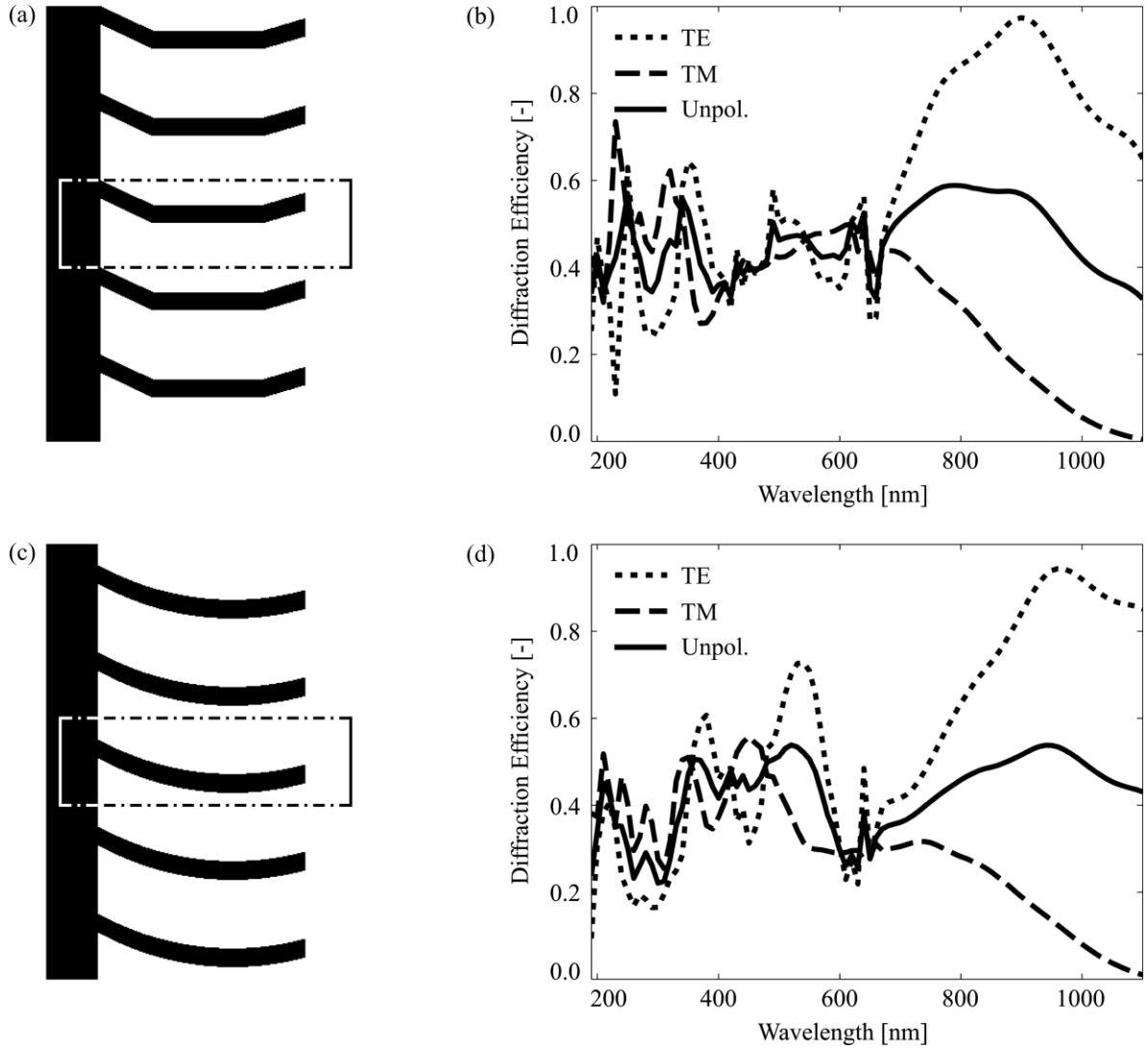

Figure 4: Two simplified dielectric transmission grating designs (a)+(c) and the resulting diffraction efficiencies (b)+(d). Simplifying the topology optimized grating design comes at the cost of reduced diffraction efficiency. The resulting diffraction efficiencies (b)+(d) for the simplified gratings for an unpolarized plane wave with wavelength between 190 nm to 1100 nm are above 30% and 20%, respectively.

From Fig. 3 we conclude that the working principle of the optimized grating structure is partly a waveguide effect and partly due to reflection at the grating ridge surface. At low wavelengths ($\lambda < 600$ nm), the structure mainly acts as a waveguide, guiding the wave in air in the direction of the -1st transmission order. As a waveguide, the grating structure works approximately equally well for the two polarizations. For longer wavelengths ($\lambda > 600$ nm), the grating structure becomes sub-wavelength and thereby non-guiding. Furthermore, the wave needs to exit the grating at increasingly greater angles (compared to the surface normal) in order to be directed towards the -1st transmission order. This is achieved mainly by reflection at the grating ridge surface. However, as a reflector, the grating structure is much more efficient for the TE polarization than the TM polarization (c.f. Figs. 3(d) and 3(g)).

The optimized design has many small details and will therefore be very challenging to fabricate. In order to both examine how important the small details are for the performance of the transmission grating and to get designs that are simpler to fabricate, two simplified gratings are constructed and shown in Fig. 4(a) and 4(c) along with the resulting diffraction efficiencies shown in Figs 4(b) and 4(d). The first simplified design is constructed in three parts, whereas the

second design is constructed as a smooth arc. Even through the two designs are simplified, they are still quite challenging to fabricate.

The simplified designs come at the cost of reduced diffraction efficiency (c.f. Figs. 4), as expected. Over the considered range of wavelengths, the diffraction efficiencies are above ~30% and ~20% for the first and second simplified design, respectively. As such, the diffraction efficiency is not too dependent on the small features of the optimized design.

5. CONCLUSION

In conclusion we have laid out a systematic procedure for designing surface relief transmission gratings with optimized transmission properties. The methodology has been used to design a grating with diffraction efficiency above 40% for unpolarized plane waves over a wavelength range from 190 nm (ultraviolet) to 1100 nm (near-infrared). The working principles of the optimized grating structure are partly a waveguide effect at short wavelengths and partly due to reflection at the grating ridge surface for longer wavelength. Two simplified gratings are constructed in order to decrease the fabrication challenges. However, the simplified designs come at the cost of reduced diffraction efficiency.

ACKNOWLEDGEMENT

We are grateful for the support from the Danish National Technology Foundation through the project "Lithography for Next Generation Micro Machined Products" and the Villum Foundation through the NextTop project.

REFERENCES

[1] Yokomari, K., "Dielectric surface-relief gratings with high diffraction efficiency," Applied Optics 23(4), 2303-2310 (1984).
[2] Moharam, M. G. and Gaylord, T. K., "Diffraction analysis of dielectric surface-relief gratings," Journal of the Optical Society of America B 72(10), 1385-1392 (1982).
[3] Clausnitzer, T., Kämpfe, T., Kley, E.-B., Tünnermann, A., Peschel, U., Tishchenko, A. V. and Parriaux, O., "An intelligible explanation of highly-efficient diffraction in deep dielectric rectangular transmission gratings," Optics Express 13(26), 10448-10456 (2005).
[4] Cao, H., Zhou C., Feng, J., Lu, P. and Ma, J., "Design and fabrication of a polarization-independent wideband transmission fused-silica grating," Applied Optics 49(21), 4108-4112 (2010).
[5] Clausnitzer, T., Limpert, J., Zöllner, K., Zellmer, H., Fuchs, H.-J., Kley, E.-B., Tünnermann, A., Jupé, M. and Ristau, D., "Highly-efficient transmission gratings in fused silica for chirped pulse amplification systems," Applied Optics 42(34), 6934-6938 (2003).
[6] Clausnitzer, T., Kley, E.-B., Fuchs, H.-J. and Tünnermann, A., "Highly-efficient polarization independent transmission gratings for pulse stretching and compression," Proc. SPIE 5252, 174-812 (2003).
[7] Wang, S., Zhou, C., Zhang, Y. and Huayi, R., "Deep-etched high-density fused-silica transmission gratings with high efficiency at a wavelength of 1550 nm," Applied Optics 45(12), 2567-2571 (2006).
[8] Sun, W., Lv, P., Zhou, C., Cao, H. and Wu, J., "Multireflection modal method for wideband fused-silica transmission gratings," Applied Optics 52(12), 2800-2807 (2013).
[9] Jing, X., Zhang, J., Jin, S., Liang, P. and Tian, Y., "Design of highly efficient transmission gratings with deep etched triangular grooves," Applied Optics 51(33), 7920-7933 (2012).
[10] Nishii, J., Kintaka, K. and Nakazawa, T., "High-efficiency transmission gratings buried in a fused-SiO_2 glass plate," Applied Optics 43(6), 1327-1330 (2004).
[11] Clausnitzer, T., Kämpfe, T., Kley, E.-B., Tünnermann, A., Tishchenko, A. V. and Parriaux, O., "Highly-dispersive dielectric transmission gratings with 100% diffraction efficiency," Optics Express 16(26), 5577-5584 (2008).
[12] Nagashima, K., Kosuge, A., Ochi, Y. and Tanaka, M., "Improvement of diffraction efficiency of dielectric transmission gratings using anti-reflection coatings," Optics Express 21(16), 18640-18645 (2013).
[13] Perry, M. D., Boyd, R. D., Britten, J. A., Decker, D. and Shore, B. W., "High-efficiency multilayer dielectric diffraction gratings," Optics Letters 20(8), 940-942 (1995).

[14] Guan, H., Chen, H., Wu, J., Jin, Y., Kong, F., Liu, S., Yi, K. and Shao, J., "High-efficiency, broad-bandwith metal/multilayer-dielectric gratings," Optics Letters 39(1), 170-173 (2014).
[15] Dobson, D. C., "Optimal design of periodic antireflective structures for the Helmholtz equation," European Journal of Applied Mathematics 4(04), 321-339 (1993).
[16] Fuchi, K., Diaz, A. R., Rothwell, E., Ouedraogo, R. and Temme, A., "Topology optimization of periodic layouts of dielectric materials," Structural and Multidisciplinary Optimization, 42(4), 483-493 (2010).
[17] Friis, K. S. and Sigmund, O., "Robust topology design of periodic grating surfaces," Journal of the Optical Soceity of America B 29(10), 2935-2943 (2012).
[18] Bendsøe, M. P. and Sigmund, O., [Topology Optimization - Theory, Methods and Applications], Springer Verlag, Berlin Heidelberg, (2004).
[19] Andkjær, J., Johansen, V. E., Friis, K. S. and Sigmund, O., "Inverse design of nanostructured surfaces for color effects," Journal of the Optical Society of America B 31(1), (2014).
[20] Jin, J., [The finite element method in electromagnetics], John Wiley & Sons, 2nd edition (2002).
[21] Taflove, A. and Hagness, S., [Computational electrodynamics: the finite-difference time-domain method], Artech House, 3rd edition (2005).
[22] Bendsøe, M. P. and Kikuchi, N., "Generating optimal topologies in structural design using a homogenization method," Computer Methods in Applied Mechanics and Engineering 71(2), 197-224 (1988).
[23] Jensen, J. S. and Sigmund, O., " Topology optimization of photonic crystal structures: A high-bandwidth low-loss T-junction waveguide," Journal of the Optical Society of America B: Optical Physics 22(6), 1191-1198 (2005).
[24] Jensen, J. S. and Sigmund, O., " Topology optimization for nano-photonics," Laser & Photonics Reviews 5(2), 308-321 (2011).
[25] Elesin, Y., Lazarov, B. S., Jensen, J. S. and Sigmund, O., "Time domain topology optimization of 3d nanophotonic devices," in review (2013).
[26] Erentok, A. and Sigmund, O., "Topology optimization of sub-wavelength antennas," IEEE Transactions on Antennas and Propagation 59(1), 58-69 (2011).
[27] Diaz, A. R. and Sigmund, O., "A topology optimization method for design of negative permeability metamaterials," Structural and Multidisciplinary Optimization 41(2), 163-177 (2010).
[28] Andkjær, J. A., Nishiwaki, S., Nomura, T. and Sigmund, O., "Topology optimization of grating couplers for the efficient excitation of surface plasmons," JOSA B 27(9), 1828-1832 (2010).
[29] Sigmund, O., "On the usefulness of non-gradient approaches in topology optimization," Structural and Multidisciplinary Optimization 43(5), 589-596 (2011).
[30] Sigmund, O., "Manufacturing tolerant topology optimization," Acta Mechanica Sinica 25(2), 227-239 (2009).
[31] Wang, F., Lazarov, B. S. and Sigmund, O., "On projection methods, convergence and robust formulations in topology optimization," Structural and Multidisciplinary Optimization 43(6), 767-784 (2011).
[32] Svanberg, K., "The Method of Moving Asymptotes – A new method for structural optimization," International Journal for Numerical Methods in Engineering 24, 359-373 (1987).